Geophysical Research Letters

RESEARCH LETTER
10.1029/2021GL097611

Flow and Bed Conditions Jointly Control Debris-Flow Erosion and Bulking

T. de Haas[1], B. W. McArdell[2], W. Nijland[1], A. S. Åberg[1,2], J. Hirschberg[2], and P. Huguenin[3]

[1]Department of Physical Geography, Utrecht University, Utrecht, The Netherlands, [2]Swiss Federal Institute for Forest, Snow and Landscape Research WSL, Birmensdorf, Switzerland, [3]Swiss Federal Institute for Forest, Snow and Landscape Research WSL, Sion, Switzerland

Key Points:

- Flow conditions and bed wetness jointly control debris-flow erosion and deposition
- Shear forces and particle-impact forces are strongly correlated and together determine erosion
- A shear-stress approach accounting for bed erodibility may be applicable for modeling debris-flow erosion

Supporting Information:

Supporting Information may be found in the online version of this article.

Correspondence to:

T. de Haas,
t.dehaas@uu.nl

Citation:

de Haas, T., McArdell, B. W., Nijland, W., Åberg, A. S., Hirschberg, J., & Huguenin, P. (2022). Flow and bed conditions jointly control debris-flow erosion and bulking. *Geophysical Research Letters*, *49*, e2021GL097611. https://doi.org/10.1029/2021GL097611

Received 22 DEC 2021
Accepted 6 MAY 2022

Abstract Debris flows can grow greatly in size and hazardous potential by eroding bed and bank materials. However, erosion mechanisms are poorly understood because debris flows are complex hybrids between a fluid flow and a moving mass of colliding particles, bed erodibility varies between events, and field measurements are hard to obtain. Here, we identify the key controls on debris-flow erosion based on a field data set that combines information on flow properties, bed conditions, and bed and bank erosion. We show that flow conditions and bed wetness jointly control debris-flow erosion. Flow conditions describing the cumulative forces exerted at the bed during an event best explain erosion. Shear forces and particle-impact forces are strongly correlated and act in conjunction in the erosion process. A shear-stress approach accounting for bed erodibility may therefore be applicable for modeling and predicting debris-flow erosion. This work provides a foundation for developing effective debris-flow erosion models.

Plain Language Summary Debris flows are water-laden masses of soil and rock, which are common geological hazards in mountainous regions worldwide. They can grow greatly in size and hazardous potential by eroding bed and bank materials. Limited understanding of these erosion processes, however, hampers effective hazard assessment and mitigation. Improving our understanding of erosion is challenging because debris flows are complex hybrids between a fluid flow and a moving mass of colliding particles, bed erodibility varies between events, and field measurements are hard to obtain. Here, we identify the key controls on debris-flow erosion based on a field data set that combines information on flow properties, bed conditions, and bed and bank erosion. We show that flow properties and bed wetness jointly control debris-flow erosion. Flow conditions that describe the cumulative forces exerted at the bed during an event best explain erosion. Shear forces and particle-impact forces are strongly correlated and act in conjunction in the erosion process. A shear-stress approach accounting for bed erodibility may therefore be applicable for modeling and predicting debris-flow erosion. This work provides a foundation for developing effective debris-flow erosion models.

1. Introduction

Debris flows are water-laden masses of soil and rock, which are common geological hazards in mountainous regions worldwide (Iverson, 1997). Over the past decades the occurrence and hazardous effects of debris flows have increased as a result of population expansion in mountainous regions, climate change, severe wildfires, and earthquakes (Cannon & DeGraff, 2009; Stoffel et al., 2014). The magnitude of debris flows can increase substantially by basal and bank erosion while it traverses from initiation zone to valley floor (Frank et al., 2015) resulting in an increase in casualties and property loss (Dowling & Santi, 2014). In addition, debris flows are increasingly recognised as one of the fundamental physical processes that transport sediment and erode bedrock in mountainous topography (McCoy, 2015; Stock and Dietrich, 2003). However, limited understanding of the processes that control debris-flow erosion currently hampers (a) accurate estimation of debris-flow magnitude and effective hazard mitigation (De Haas et al., 2020; Dietrich & Krautblatter, 2019) and (b) understanding and modeling of landscape evolution (Penserini et al., 2017; Tucker & Hancock, 2010).

Observations show that erosion volumes may strongly vary between debris-flow events: some flows increase >50 times their initial volume (Hungr et al., 2005), while others barely increase in size (Santi et al., 2008), and we currently lack the means to explain these contrasting pathways of development. Understanding debris-flow erosion is notoriously complicated for a number of reasons: (a) debris flows are complex hybrids between a fluid flow and a moving mass of colliding particles that may vary greatly in composition, such that both shear and

impact forces may contribute to erosion, but how these forces interact remains partly unclear (De Haas & van Woerkom, 2016; Hsu et al., 2008; Roelofs et al., 2022; Schürch et al., 2011); (b) bed erodibility may strongly vary, as it depends on a combination of grain-size distribution, moisture content, and hardness (e.g., soft sediment vs. bedrock) (Iverson et al., 2011; Stock & Dietrich, 2003; Zheng et al., 2021); (c) in-situ flow measurements are cost- and time-demanding because of the destructive and infrequent nature of debris flows and the rough terrain in which they occur.

Field data on debris-flow erosion are scarce, often limited to single debris-flow events (Dietrich & Krautblatter, 2019), based on local point or cross-section measurements (Berger et al., 2011; McCoy et al., 2012), and its analysis limited by unknown or irreproducible boundary conditions (Iverson et al., 2010). There has been a recent increase in the number of numerical models incorporating erosion (Frank et al., 2015; McDougall & Hungr, 2005; Pudasaini & Krautblatter, 2021), but the inconsistency in erosion rate equations as a result of a lack of a unified theory still results in a disparity of model outcomes. At the same time, erosion is still neglected in many other models actively used for hazard assessment and mitigation (Castelli et al., 2017; Luna et al., 2014), which leads to systematic underestimation of debris-flow propagation, runout, and impact (Dietrich & Krautblatter, 2019; Gregoretti et al., 2019). To (a) further our understanding of debris-flow erosion, (b) extrapolate findings from theoretical considerations (Iverson & Ouyang, 2015) and physical-scale experiments (Lanzoni et al., 2017) to complex field environments, and (c) to validate and calibrate theoretical and numerical models, there is thus a need for comprehensive field datasets and analyses that combine joint measurements of flow and bed conditions with measurements of bed and bank erosion.

In this study we combine detailed in-situ measurements of debris-flow conditions, antecedent rainfall, and high-resolution measurements of topographic channel change for 13 debris flows in the Illgraben torrent in the southwestern Swiss Alps. With this data we identify the processes that govern debris-flow erosion and deposition, and demonstrate that flow and bed conditions jointly control debris-flow erosion, shear and impact forces are strongly related and together cause debris-flow erosion, and although erosion at the flow front may be most intense the work done by the body and tail of the flow cannot be neglected.

2. The Illgraben Torrent and Measurement Station

The Illgraben torrent has a long history of debris flows and debris floods with multiple events each year (Bennett et al., 2014; Hirschberg et al., 2021). Debris flows are generally triggered by intense rainfall during summer storms between May and October. The flows originate from a catchment that extends from the top of the Illhorn mountain (elevation 2,716 m a.s.l.) to the Rhône River on the valley floor (610 m a.s.l.), and which consists of dolomites, quartzite, conglomerates, and calcareous sedimentary rocks (McArdell and Sartori, 2021).

This study focusses on the lowest 800 m of the channel (Figure 1), which has an average gradient of ∼4°, an average width of ∼25 m, steep banks, is incised into unconsolidated alluvial fan sediments, and contains three check dams. Previous work has shown that debris flows may substantially erode this channel while erosion by floods is negligible (Berger, 2010). Debris-flow erosion is typically more pronounced on the steeper slopes of watersheds (e.g., Imaizumi et al., 2019), and a number of other debris flows have been observed to be net depositional on relatively gentle slopes such as that of our study reach (Berti et al., 1999; Rengers et al., 2021; Simoni et al., 2020)—it is likely that this variability results from differences in flow rheology. The check dams in the study reach affect bed erosion, leading to a general pattern of relatively large amounts of erosion or deposition downstream of check dams moving to a (nearly) fixed bed level at check dams (De Haas et al., 2020).

About 120 m upstream of the confluence with the Rhône River an automated observation station is operated by the Swiss Federal Institute for Forest Snow and Landscape Research (WSL), which records flow-front velocity, flow depth, bulk density, normal and shear forces, and seismic ground velocity, and collects imagery (Hürlimann et al., 2003; McArdell et al., 2007). From these observations, it is possible to calculate the front discharge of a debris flow and to estimate its volume (Schlunegger et al., 2009). Combined with drone-based structure-from-motion to generate high-resolution and high-accuracy Digital Elevation Models (DEMs) (De Haas et al., 2020, 2021), this presents an opportunity to identify the factors controlling debris-flow erosion in vivo.

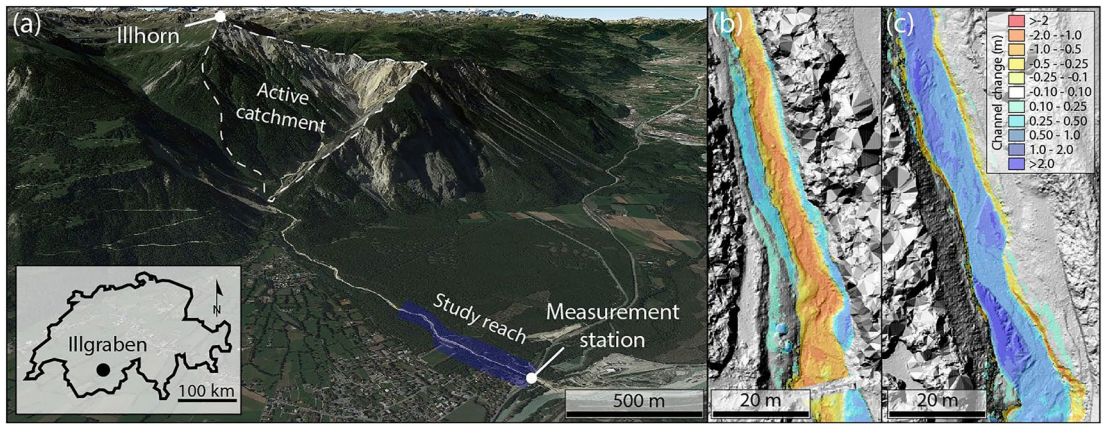

Figure 1. (a) Overview of the Illgraben catchment, fan, channel, and location of the study reach and measurement station. (b) Example of channel-bed elevation change as a result of debris-flow 12 (07 August 2021), which was net erosional. (c) Example of channel-bed elevation change as a result of debris-flow 11 (16 July 2021), which was net depositional.

3. Materials and Methods

3.1. Digital Elevation Models

Digital elevation models (DEMs) of the study reach were made through structure-from-motion with Agisoft Metashape Pro. The 2019 imagery was captured with a DJI Mavic 2 Pro. These surveys were co-aligned and include 29 ground control points (GCPs) to optimize absolute and relative accuracies (data set and further details are published in De Haas et al., 2021). For the 2020 and 2021 surveys a DJI Phantom 4 real-time kinematic (RTK) was used. The RTK technology in this drone ensured much higher accuracies (Nota et al., 2022). Therefore, these surveys were processed individually including ∼10 GCPs. The absolute and relative accuracies of the DEMs are <10 cm in xy and z directions, and in the order of 5 cm for most surveys. To filter erroneous points and overhanging vegetation from the dense point clouds we adopted the approach of De Haas et al. (2020) using LAStools (rapidlasso GmbH). This procedure removes low noise (i.e., noise below the actual ground surface) and filters overhanging vegetation, while retaining natural detail in the channel, and mostly avoids clipping at steep sections at the channel banks and check dams.

3.2. Quantification of Erosion and Deposition

We quantified net channel-bed elevation change following the method by De Haas et al. (2020). DEMs of difference were generated by subtracting the pre-flow DEM from the post-flow DEM. We manually digitized the flow extent using mudlines and levees left behind by the debris flows. We used this extent to clip out the DEMs of difference, such that we only consider topographic changes in the area affected by a debris flow. For the quantification of channel-bed elevation change volumes, we excluded areas within 2 m of check dams, because tiny offsets in check dam location could otherwise yield very large, and incorrect, local elevation changes.

3.3. Debris-Flow Characteristics

Debris-flow characteristics are measured by the Swiss Institute for Forest, Snow and Landscape Research (WSL) at a station at check dam 29 in the Illgraben channel, located approximately 120 m upstream of the confluence with the Rhône River on the valley floor (Figure 1). The measurement station includes (a) a laser sensor that measures the top of the flow (flow depth); (b) a 8 m^2 force plate installed flush with the bottom of the check dam, with normal force sensors under each corner registering normal stress and normal-stress fluctuations, and horizontal force sensors at the two upstream corners of the plate registering shear stress and shear-stress fluctuations; (c) and a geophone connected to the force plate which measures the velocity of the force plate in vertical direction. The laser and radar devices measuring flow depth are mounted above the force plate in the check dam, where there is no erosion and little tendency for deposition. The combined flow depth and normal force measurements

Table 1
Summary of Flow Characteristics, Antecedent Rainfall, and Channel-Bed Elevation Change

	Date	H_{front}[a] (m)	v_{front}[b] (m s^{-1})	Q_{peak}[c] (m^3 s^{-1})	τ_{front}[d] (kPa)	ρ[e] (kg m^{-3})	V[f] (m^3)	cum.τ[g] (kPa s)	SE[h] (m^2 s^{-2})	AR[i] (mm)	Erosion[j] (m^3 m^{-1})
1	2019-06-21	2.59	6.62	147.61	4.39	1,870	83,123	4,240	1.6×10^{-3}	17.1	−1.75
2	2019-07-15	0.54	3.39	16.54	0.98	2,191	9,869	584	4.6×0^{-5}	6.5	0.33
3	2019-07-26	1.05	8.69	93.26	2.15	2,223	29,077	3,561	2.0×10^{-4}	18.8	−1.65
4	2019-08-11	1.8	6.95	95.63	4.12	2,323	70,705	7,185	5.2×10^{-4}	17.6	−0.69
5	2019-08-20	0.44	0.89	8.06	0.75	2,031	21,031	1,881	1.4×10^{-4}	4.4	−0.28
6	2020-06-29	1.23	1.23	8.74	2.18	2,066	3,816	3,703	3.0×10^{-4}	9.4	0.06
7	2020-08-17	0.27	0.49	3.31	0.63	2,240	14,042	1,826	7.2×10^{-5}	2.6	2.66
8	2020-08-30	0.98	0.73	13.05	1.56	1,777	109,840	11,531	1.1×10^{-3}	10.4	−6.66
9	2021-06-05	0.24	1.96	6.83	0.37	1,602	625	737	-	8.7	−0.71
10	2021-07-06	2.5	8.69	186.61	3.57	1,605	58,498	2,368	4.2×10^{-4}	9.4	−1.40
11	2021-07-16	1.61	2.78	60.7	2.65	1,916	86,989	12,900	8.2×10^{-4}	7.3	2.70
12	2021-08-07	1.51	2.32	41.19	2.48	1,884	39,738	7,428	6.7×10^{-4}	12.2	−0.78
13	2021-09-19	0.86	1.25	10.67	1.38	1,697	9,084	3,101	3.7×10^{-4}	12.0	−0.38

[a]Frontal flow depth. [b]Front velocity. [c]Peak discharge. [d]Frontal shear stress. [e]Mean bulk density. [f]Flow volume. [g]Cumulative shear stress. [h]Seismic energy. [i]3 hr antecedent rainfall. [j]Net channel-bed elevation change.

allow for calculation of the bulk density of the flows. Flow front and surge velocities are estimated from the travel time along the 120 m channel stretch between CD28 and CD29 at the measurement station (McArdell, 2016; McArdell et al., 2007). From these observations, it is possible to calculate the frontal discharge of a debris flow and to estimate total flow volume. The volume of each debris flow (Table 1) was calculated as the product of the flow velocity and the cross-sectional area, integrated over the duration of the flow (Schlunegger et al., 2009).

3.4. Antecedent Rainfall

Antecedent rainfall is measured at the Swiss Federal Office of Meteorology and Climatology (MeteoSwiss) station located near Crans-Montana at an elevation of 1,423 m above sea level, approximately 11 km from the Illgraben torrent (lat/lon 46.298806°/7.460814°). The antecedent rainfall is defined as the cumulative amount of rainfall in a given period preceding debris-flow arrival at the measurement station.

4. Factors Controlling Debris-Flow Erosion

We have measured the pre-flow and post-flow topography of 13 debris flows over the period 2019–2021. These flows ranged in size from 600 to 87,000 m^3, had frontal flow velocities between 0.5 and 9 m s^{-1}, frontal flow depths ranging from 0.25 to 3 m, and mean bulk densities between 1,600 and 2,300 kg m^{-3} (Table 1). There is a wide variety in the hydrographs and flow regimes, ranging from (a) single-surge flows with a steep front followed by a tapering tail to (b) flows with indistinct fronts and (c) to multi-surge events. Moreover, flows range from having well-developed to poorly-developed coarse-grained fronts, and flows can have hyperconcentrated or muddy-viscous bodies and tails (Table S4; Figures S1, S3–S15 in Supporting Information S1).

To determine the factors controlling debris-flow erosion and deposition, we compare the net channel-bed elevation change over a reach of 800 m upstream of the measurement station with measured flow properties and antecedent rainfall (Figure 1). We express channel-bed elevation change in m^3 per m of channel length in the downstream direction. We assume that the flow properties, as measured at the station, were approximately steady over the study reach, because it is relatively straight, channel slope and width are relatively constant, and the volume of eroded or deposited sediment over this reach was limited to a few percent of the total volume of the flows.

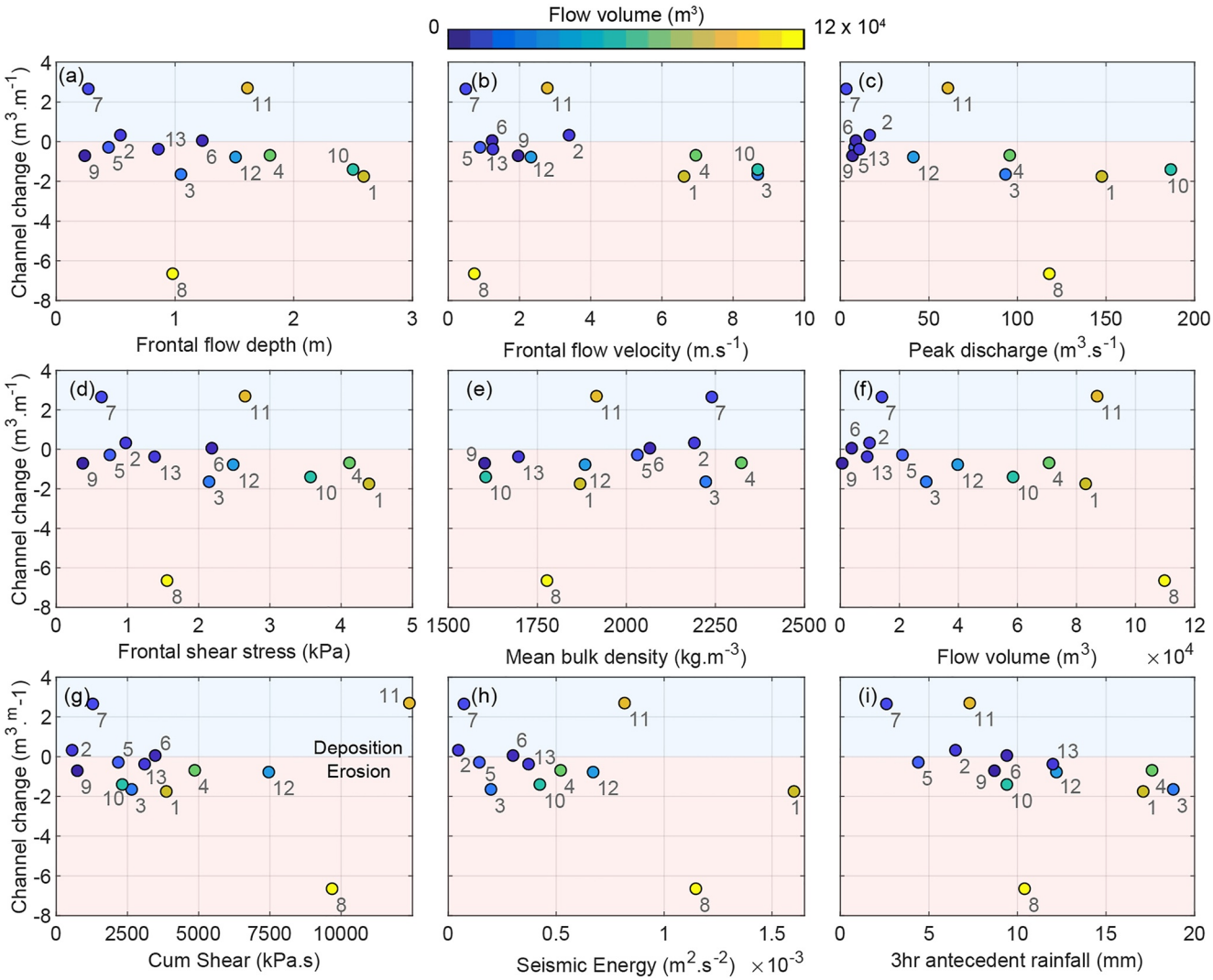

Figure 2. Flow properties (a–h) and antecedent rainfall (i) versus and channel-bed elevation change. See Table S1 in Supporting Information S1 for correlation coefficients.

Multiple flow properties have statistically significant correlations with channel-bed elevation change when excluding one or two common outliers (Figure 2; Table S1 in Supporting Information S1). These outliers, events 8 and 11, are the result of a very long flow duration and limited antecedent rainfall, respectively, as explained at the end of this section. The strongest correlations in our data set (excluding event 11) are those between channel-bed elevation change and flow properties that consider debris-flow activity over time, such as flow volume (R^2 = 0.58), cumulative shear stress (R^2 = 0.55), and seismic energy (SE) (squared integrated ground velocity amplitude (Schimmel et al., 2021)) (R^2 = 0.41) (Figures 2f–2h, Table S1 in Supporting Information S1). Statistically significant relations are also found for frontal flow properties when we exclude events 8 and 11 (Figures 2a–2d): Frontal flow depth (R^2 = 0.39), frontal flow velocity (R^2 = 0.46), and frontal discharge (R^2 = 0.42). The correlation between frontal shear stress, calculated as $\tau = rgHS$, wherein r = flow density, g = gravitational acceleration, H = frontal flow depth, S = channel inclination, and channel-bed elevation change is marginally significant with a p-value of 0.06 and R^2 of 0.35. We find no significant trend between mean bulk density and channel-bed elevation change (Figure 2e), although some high-density flows seem to have a higher tendency toward deposition which would agree with previous studies which have suggested that erosion is higher in more dilute flows where sediment concentrations are below an equilibrium value (Egashira et al., 2001; Fagents & Baloga, 2006; Pudasaini & Krautblatter, 2021; Takahashi, 1981).

We further find significant positive correlations between antecedent rainfall over a period of 2–3 hr, when excluding event 8 ($R^2 \approx 0.47$; $p \approx 0.01$) (Figure 2i; Figure S2; Table S1 in Supporting Information S1). For a period of 4–12 hr, the trend decreases in strength and becomes marginally significant, while beyond a period of 12 hr there is no significant trend. Similarly, we find no significant trend for 1 hr antecedent rainfall. We attribute the strong correlation between short-term antecedent rainfall and channel-bed elevation change to an increase in bed moisture with increasing antecedent moisture. Short-term antecedent rainfall induces runoff in the torrent which wets the bed, and thereby increases its erodibility (Iverson et al., 2011).

We find that events 8 and 11 act as outliers when frontal flow properties are considered, event 11 acts as an outlier when flow properties that consider debris-flow activity over time are considered, and that event 8 acts as an outlier when antecedent rainfall is considered. These outliers can be physically explained. Event 8, while having a relatively modest flow front, was of very long duration with a larger and faster moving second main surge, with a velocity of ∼6 m s^{-1} and a frontal flow depth of ∼2 m (Table 1; Figure S10 in Supporting Information S1). As a result, channel-bed elevation change is strongly underestimated when frontal flow properties are considered, while it fits the trend when flow properties are integrated over time. During event 11, on the other hand, antecedent rainfall was limited, especially 3–9 hr prior to the event (Figure S2 in Supporting Information S1). Therefore, the bed moisture content was likely very low resulting in deposition where erosion would have been expected based on flow properties alone.

5. Discussion

5.1. Shear Forces Versus Impact Forces

Because debris flows are high-density mixtures, erosion has been attributed to both basal shear forces (Frank et al., 2015; Hungr et al., 2005; Schürch et al., 2011) and impact forces (Berger et al., 2011; Hsu et al., 2008; Stock and Dietrich, 2006), but how these forces interact in the bed-erosion process remains largely unknown (De Haas & van Woerkom, 2016; Kavinkumar et al., 2021; Roelofs et al., 2022). The composition of debris flows can vary substantially ranging from mudflows and lahars with a high fraction of fine particles (clay, silt, sand) to granular flows with a high fraction of coarse particles with diameters that may exceed a meter (e.g., Kaitna et al., 2016). Moreover, their composition may also strongly differ within an event—typically a coarse-grained flow front or surges with a low water content are followed by a finer-grained and more fluidal flow body (e.g., Iverson, 1997; McArdell et al., 2007). Therefore, the relative importance of shear and impact forces for debris-flow erosion may differ between and within flows. The forces measured at the base of a debris flow can be partitioned into mean forces and fluctuations around the mean. These distinct types of forces are associated with distinct mechanisms. Hsu et al. (2008, 2014) show that wear by sliding varies with the mean normal and shear forces and wear by particle impacts varies with the fluctuating force components (Bagnold, 1954; Stock and Dietrich, 2006).

To shed light on how shear and impact forces interact and control erosion we compare measured shear forces with measured fluctuating forces, expressed as normal-force fluctuations captured by the force plate and as ground velocity captured by a geophone connected to the force plate (Figure 3). We find that mean shear forces and force fluctuations are strongly correlated for the flows in our data set, similar to small-scale experimental debris flows (Roelofs et al., 2022). An increase in shear forces leads to an increase in force fluctuations. Moreover, for most flows the ratio between shear forces and fluctuating forces is similar, although we do observe that relatively muddy and viscous events (e.g., events 11–12) have relatively small force fluctuations, while the force fluctuations in the relatively granular and coarse-grained event 1 are relatively large (Figure 3).

We find no increase in erosiveness for event 1, despite having large force fluctuations and large total SE (Figure 2h). In contrast, the amount of erosion in event 1 predominantly scales with the cumulative shear exerted on the bed by the debris flow (Figure 2g), which suggests that shear forces dominate the erosion process, at least on the unconsolidated bed of the lower parts of the Illgraben torrent. The overall strong correspondence between shear forces and fluctuations further explain the statistically significant trends found for both cumulative shear force and SE with bed erosion. A major implication of this finding is that erosion may be effectively predicted from either shear forces or impact forces. Moreover, it may open up a wealth of data for studying debris-flow

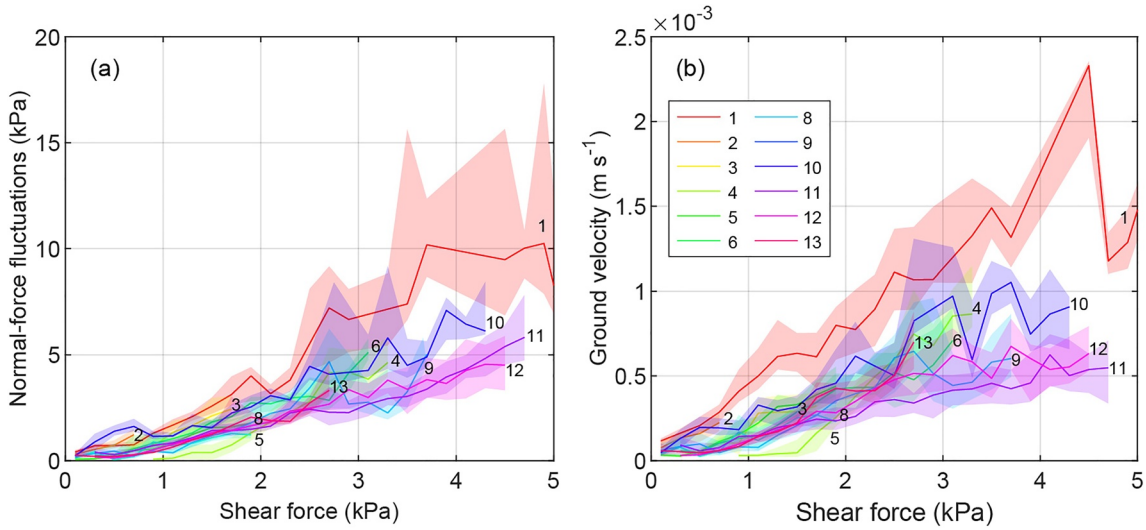

Figure 3. Comparison of shear forces versus fluctuating forces. (a) Shear force versus normal force fluctuations. (b) Shear force versus ground velocity. The solid lines indicate the median and the colored bands denote the 25th–75th percentile range in 0.2 kPa shear force bins. The numbers correspond to the debris-flow events listed in Table 1.

erosion by exploiting the large number of geophone measurements which are currently predominantly used for early warning (e.g., Hürlimann et al., 2019; Zhang et al., 2021).

5.2. Front, Body, or Tail?

There is no consensus in previous studies on whether erosion predominantly takes place during passage of the flow front which generally has a high flow depth and a large concentration of large particles (Berger et al., 2011; Schürch et al., 2011), or whether erosion is substantial during both the passage of the flow front, body, and tail (McCoy et al., 2012; Rickenmann et al., 2003). Although we acknowledge that this may differ between flows and sites, our results show that overall the cumulative work of the debris flows exerted at the bed best explains the observed channel-bed elevation change (Figure 2; Table 1 in Supporting Information S1). While we find statistically significant relations for frontal flow properties with erosion (Figures 1a–1d) and cumulative forces with erosion (Figures 1f–1h), the correlations for the latter are stronger. It is important to note that both are related in that the largest flows generally also have the largest flow fronts (Tables S2 and S3 in Supporting Information S1). It is therefore likely that erosion at the flow front is most intense (cf., Berger et al., 2011), but our data shows that erosion in the body and tail of the flow cannot be neglected.

5.3. Implications for Erosion Prediction and Modeling

Our observations highlight the complexity of debris-flow erosion. We show that both flow and bed conditions significantly affect erosion and thereby flow-volume growth, but that none of the variables has a very high predictive capacity on its own. Both flow and bed conditions should therefore be considered in prediction and modeling of debris-flow erosion, in contrast to previous work which predominantly attributes erosion to either flow properties (Schürch et al., 2011) or bed wetness (McCoy et al., 2012). The material eroded by a debris flow depends most strongly on the cumulative forces exerted on the bed during the entire event in our data set. Accurate predictions should therefore account for the forces exerted on the channel bed during the entire event, which many modern debris-flow models do (e.g., Baggio et al., 2021; Frank et al., 2015; Pudasaini & Krautblatter, 2021), and bed-erodibility conditions which are less commonly included in modern debris-flow models. Our finding that shear forces and impact forces are strongly correlated does increase the feasibility of modeling erosion in debris flows because it shows that a shear stress approach accounting for bed erodibility may suffice to model debris-flow erosion—at least in unconsolidated channels. Our work further provides key guidelines and data against which to validate and calibrate debris-flow erosion models.

6. Conclusions

We have combined detailed flow measurements, rainfall data, and high-resolution measurements of channel-bed erosion and deposition for 13 debris flows in the Illgraben (CH), to identify the key controls on debris-flow erosion and deposition.

The data show that both flow conditions and bed wetness control erosion and deposition occurrence and quantities. Flow conditions that describe the cumulative forces exerted at the bed over the full event (flow volume, cumulative shear stress, and SE) have the strongest correlations with measured erosion and deposition. However, we also find statistically significant correlations between erosion and deposition and frontal flow properties, including frontal velocity, flow depth, shear stress, and peak discharge. Antecedent rainfall over a period of 2–3 hr prior to the debris-flow events strongly correlates to erosion and deposition, while the correlation decreases in strength and diminishes toward shorter and longer time periods of antecedent moisture.

Shear forces and particle-impact forces are strongly correlated and jointly erode the bed, that is, flows with higher shear forces also have higher impact forces. This suggests that applying a shear-stress approach accounting for bed erodibility may therefore be applicable for modeling and predicting debris-flow erosion, as it will also largely incorporate the impact forces. The work and data presented here provides key input for model development by identifying key correlations of flow and bed conditions with erosion that models should oblige.

Data Availability Statement

Topographic and debris-flow data can be accessed at https://doi.org/10.24416/UU01-XXASOM.

Acknowledgments
This work was supported by the Netherlands Organisation for Scientific Research (NWO) (Grant 016.Veni.192.001 to TdH).

References

Baggio, T., Mergili, M., & D'Agostino, V. (2021). Advances in the simulation of debris flow erosion: The case study of the Rio Gere (Italy) event of the 4th August 2017. *Geomorphology*, *381*, 107664. https://doi.org/10.1016/j.geomorph.2021.107664

Bagnold, R. A. (1954). Experiments on a gravity-free dispersion of large solid spheres in a Newtonian fluid under shear. *Proceedings of the Royal Society of London. Series A. Mathematical and Physical Sciences*, *225*, 49–63.

Bennett, G. L., Molnar, P., McArdell, B. W., & Burlando, P. (2014). A probabilistic sediment cascade model of sediment transfer in the Illgraben. *Water Resources Research*, *50*(2), 1225–1244. https://doi.org/10.1002/2013wr013806

Berger, C. (2010). *Debris flow entrainment and sediment transfer processes at the Illgraben catchment, Switzerland*. PhD thesis, University of Bern.

Berger, C., McArdell, B. W., & Schlunegger, F. (2011). Direct measurement of channel erosion by debris flows, Illgraben, Switzerland. *Journal of Geophysical Research*, *116*(F1), F01002. https://doi.org/10.1029/2010jf001722

Berti, M., Genevois, R., Simoni, A., & Tecca, P. R. (1999). Field observations of a debris flow event in the Dolomites. *Geomorphology*, *29*(3–4), 265–274. https://doi.org/10.1016/s0169-555x(99)00018-5

Cannon, S. H., & DeGraff, J. (2009). The increasing wildfire and post-fire debris-flow threat in Western USA, and implications for consequences of climate change. *Landslides–disaster risk reduction* (pp. 177–190). Springer.

Castelli, F., Freni, G., Lentini, V., & Fichera, A. (2017). Modelling of a debris flow event in the Enna area for hazard assessment. *Procedia Engineering*, *175*, 287–292. https://doi.org/10.1016/j.proeng.2017.01.026

De Haas, T., Nijland, W., De Jong, S. M., & McArdell, B. W. (2020). How memory effects, check dams, and channel geometry control erosion and deposition by debris flows. *Scientific Reports*, *10*, 1–8. https://doi.org/10.1038/s41598-020-71016-8

De Haas, T., Nijland, W., McArdell, B. W., & Kalthof, M. W. (2021). Case report: Optimization of topographic change detection with UAV structure-from-motion photogrammetry through survey co-alignment. *Frontiers in Remote Sensing*, *2*, 5. https://doi.org/10.3389/frsen.2021.626810

De Haas, T., & van Woerkom, T. (2016). Bed scour by debris flows: Experimental investigation of effects of debris-flow composition. *Earth Surface Processes and Landforms*, *41*(13), 1951–1966. https://doi.org/10.1002/esp.3963

Dietrich, A., & Krautblatter, M. (2019). Deciphering controls for debris-flow erosion derived from a LiDAR-recorded extreme event and a calibrated numerical model (Roßbichelbach, Germany). *Earth Surface Processes and Landforms*, *44*(6), 1346–1361. https://doi.org/10.1002/esp.4578

Dowling, C. A., & Santi, P. M. (2014). Debris flows and their toll on human life: A global analysis of debris-flow fatalities from 1950 to 2011. *Natural Hazards*, *71*(1), 203–227. https://doi.org/10.1007/s11069-013-0907-4

Egashira, S., Honda, N., & Itoh, T. (2001). Experimental study on the entrainment of bed material into debris flow. *Physics and Chemistry of the Earth—Part C: Solar, Terrestrial & Planetary Science*, *26*(9), 645–650. https://doi.org/10.1016/s1464-1917(01)00062-9

Fagents, S. A., & Baloga, S. M. (2006). Toward a model for the bulking and debulking of lahars. *Journal of Geophysical Research*, *111*(B10), B10201. https://doi.org/10.1029/2005jb003986

Frank, F., McArdell, B. W., Huggel, C., & Vieli, A. (2015). The importance of entrainment and bulking on debris flow runout modeling: Examples from the Swiss Alps. *Natural Hazards and Earth System Sciences*, *15*(11), 2569–2583. https://doi.org/10.5194/nhess-15-2569-2015

Gregoretti, C., Stancanelli, L. M., Bernard, M., Boreggio, M., Degetto, M., & Lanzoni, S. (2019). Relevance of erosion processes when modelling in-channel gravel debris flows for efficient hazard assessment. *Journal of Hydrology*, *568*, 575–591. https://doi.org/10.1016/j.jhydrol.2018.10.001

Hirschberg, J., Badoux, A., McArdell, B. W., Leonarduzzi, E., & Molnar, P. (2021). Evaluating methods for debris-flow prediction based on rainfall in an Alpine catchment. *Natural Hazards and Earth System Sciences*, *21*(9), 2773–2789. https://doi.org/10.5194/nhess-21-2773-2021

Hsu, L., Dietrich, W. E., & Sklar, L. S. (2008). Experimental study of bedrock erosion by granular flows. *Journal of Geophysical Research*, *113*(F2), F02001. https://doi.org/10.1029/2007jf000778

Hsu, L., Dietrich, W. E., & Sklar, L. S. (2014). Mean and fluctuating basal forces generated by granular flows: Laboratory observations in a large vertically rotating drum. *Journal of Geophysical Research: Earth Surface*, *119*(6), 1283–1309. https://doi.org/10.1002/2013jf003078

Hungr, O., McDougall, S., & Bovis, M. (2005). Entrainment of material by debris flows. *Debris-flow hazards and related phenomena* (pp. 135–158). Springer Berlin Heidelberg.

Hürlimann, M., Coviello, V., Bel, C., Guo, X., Berti, M., Graf, C., et al. (2019). Debris-flow monitoring and warning: Review and examples. *Earth-Science Reviews*, *199*, 102981. https://doi.org/10.1016/j.earscirev.2019.102981

Hürlimann, M., Rickenmann, D., & Graf, C. (2003). Field and monitoring data of debris-flow events in the Swiss Alps. *Canadian Geotechnical Journal*, *40*(1), 161–175. https://doi.org/10.1139/t02-087

Imaizumi, F., Masui, T., Yokota, Y., Tsunetaka, H., Hayakawa, Y. S., & Hotta, N. (2019). Initiation and runout characteristics of debris flow surges in Ohya landslide scar, Japan. *Geomorphology*, *339*, 58–69. https://doi.org/10.1016/j.geomorph.2019.04.026

Iverson, R. M. (1997). The physics of debris flows. *Reviews of Geophysics*, *35*(3), 245–296. https://doi.org/10.1029/97rg00426

Iverson, R. M., Logan, M., LaHusen, R. G., & Berti, M. (2010). The perfect debris flow? Aggregated results from 28 large-scale experiments. *Journal of Geophysical Research*, *115*(F3), F03005. https://doi.org/10.1029/2009jf001514

Iverson, R. M., & Ouyang, C. (2015). Entrainment of bed material by Earth-surface mass flows: Review and reformulation of depth-integrated theory. *Reviews of Geophysics*, *53*(1), 27–58. https://doi.org/10.1002/2013rg000447

Iverson, R. M., Reid, M. E., Logan, M., LaHusen, R. G., Godt, J. W., & Griswold, J. P. (2011). Positive feedback and momentum growth during debris-flow entrainment of wet bed sediment. *Nature Geoscience*, *4*(2), 116–121. https://doi.org/10.1038/ngeo1040

Kaitna, R., Palucis, M. C., Yohannes, B., Hill, K. M., & Dietrich, W. E. (2016). Effects of coarse grain size distribution and fine particle content on pore fluid pressure and shear behavior in experimental debris flows. *Journal of Geophysical Research: Earth Surface*, *121*(2), 415–441. https://doi.org/10.1002/2015jf003725

Kavinkumar, C., Sureka, S., Pillai, R. J., & Mudavath, H. (2021). Influence of erodible layer on granular column collapse using discrete element analysis. *Geomechanics and Geoengineering*, 1–13. https://doi.org/10.1080/17486025.2021.1928759

Lanzoni, S., Gregoretti, C., & Stancanelli, L. M. (2017). Coarse-grained debris flow dynamics on erodible beds. *Journal of Geophysical Research: Earth Surface*, *122*(3), 592–614. https://doi.org/10.1002/2016jf004046

Luna, B. Q., Quan Luna, B., Blahut, J., Camera, C., van Westen, C., Apuani, T., et al. (2014). Physically based dynamic run-out modelling for quantitative debris flow risk assessment: A case study in Tresenda, northern Italy. *Environmental Earth Sciences*, *72*, 645–661.

McArdell, B. W. (2016). Field measurements of forces in debris flows at the Illgraben: Implications for channel-bed erosion. *International Journal of Erosion Control Engineering*, *9*(4), 194–198. https://doi.org/10.13101/ijece.9.194

McArdell, B. W., Bartelt, P., & Kowalski, J. (2007). Field observations of basal forces and fluid pore pressure in a debris flow. *Geophysical Research Letters*, *34*(7), L07406. https://doi.org/10.1029/2006gl029183

McArdell, B. W., & Sartori, M. (2021). The Illgraben torrent system. In *Landscapes and landforms of Switzerland* (pp. 367–378). Springer.

McCoy, S. W. (2015). Infrequent, large-magnitude debris flows are important agents of landscape change. *Geology*, *43*(5), 463–464. https://doi.org/10.1130/focus052015.1

McCoy, S. W., Kean, J. W., Coe, J. A., Tucker, G. E., Staley, D. M., & Wasklewicz, T. A. (2012). Sediment entrainment by debris flows: In situ measurements from the headwaters of a steep catchment. *Journal of Geophysical Research*, *117*(F3), F03016. https://doi.org/10.1029/2011jf002278

McDougall, S., & Hungr, O. (2005). Dynamic modelling of entrainment in rapid landslides. *Canadian Geotechnical Journal*, *42*(5), 1437–1448. https://doi.org/10.1139/t05-064

Nota, E. W., Nijland, W., & de Haas, T. (2022). Improving UAV-SfM time-series accuracy by co-alignment and contributions of ground control or RTK postioning. *International Journal of Applied Earth Observation and Geoinformation*, *109*, 102772.

Penserini, B. D., Roering, J. J., & Streig, A. (2017). A morphologic proxy for debris flow erosion with application to the earthquake deformation cycle, Cascadia Subduction Zone, USA. *Geomorphology*, *282*, 150–161. https://doi.org/10.1016/j.geomorph.2017.01.018

Pudasaini, S. P., & Krautblatter, M. (2021). The mechanics of landslide mobility with erosion. *Nature Communications*, *12*(1), 1–15. https://doi.org/10.1038/s41467-021-26959-5

Rengers, F. K., McGuire, L. A., Kean, J. W., Staley, D. M., Dobre, M., Robichaud, P. R., & Swetnam, T. (2021). Movement of sediment through a burned landscape: Sediment volume observations and model comparisons in the San Gabriel Mountains, California, USA. *Journal of Geophysical Research: Earth Surface*, *126*(7), e2020JF006053. https://doi.org/10.1029/2020jf006053

Rickenmann, D., Weber, D., & Stepanov, B. (2003). Erosion by debris flows in field and laboratory experiments. *Debris flow hazards mitigation: Mechanics, prediction, and assessment* (pp. 883–894). Millpress.

Roelofs, L., Colucci, P., & deHaas (2022). *How debris-flow composition affects bed erosion quantity and mechanisms: An experimental assessment. Earth Surface Processes and Landforms, 1–19*. https://doi.org/10.1002/esp.5369

Santi, P. M., Higgins, J. D., Cannon, S. H., & Gartner, J. E. (2008). Sources of debris flow material in burned areas. *Geomorphology*, *96*(3–4), 310–321. https://doi.org/10.1016/j.geomorph.2007.02.022

Schimmel, A., Coviello, V., & Comiti, F. (2021). Debris-flow velocity and volume estimations based on seismic data. *Natural Hazards and Earth System Sciences Discussions*, 1–21.

Schlunegger, F., Badoux, A., McArdell, B. W., Gwerder, C., Schnydrig, D., Rieke-Zapp, D., & Molnar, P. (2009). Limits of sediment transfer in an alpine debris-flow catchment, Illgraben, Switzerland. *Quaternary Science Reviews*, *28*(11–12), 1097–1105. https://doi.org/10.1016/j.quascirev.2008.10.025

Schürch, P., Densmore, A. L., Rosser, N. J., & McArdell, B. W. (2011). Dynamic controls on erosion and deposition on debris-flow fans. *Geology*, *39*(9), 827–830. https://doi.org/10.1130/g32103.1

Simoni, A., Bernard, M., Berti, M., Boreggio, M., Lanzoni, S., Stancanelli, L. M., & Gregoretti, C. (2020). Runoff-generated debris flows: Observation of initiation conditions and erosion–deposition dynamics along the channel at Cancia (eastern Italian Alps). *Earth Surface Processes and Landforms*, *45*(14), 3556–3571. https://doi.org/10.1002/esp.4981

Stock, J., & Dietrich, W. E. (2003). Valley incision by debris flows: Evidence of a topographic signature. *Water Resources Research*, *39*(4), C81089. https://doi.org/10.1029/2001wr001057

Stock, J. D., & Dietrich, W. E. (2006). Erosion of steepland valleys by debris flows. *The Geological Society of America Bulletin*, *118*(9–10), 1125–1148. https://doi.org/10.1130/b25902.1

Stoffel, M., Mendlik, T., Schneuwly-Bollschweiler, M., & Gobiet, A. (2014). Possible impacts of climate change on debris-flow activity in the Swiss Alps. *Climatic Change*, *122*(1–2), 141–155. https://doi.org/10.1007/s10584-013-0993-z

Takahashi, T. (1981). Debris flow. *Annual Review of Fluid Mechanics*, *13*(1), 57–77. https://doi.org/10.1146/annurev.fl.13.010181.000421

Tucker, G. E., & Hancock, G. R. (2010). Modelling landscape evolution. *Earth Surface Processes and Landforms*, *35*(1), 28–50. https://doi.org/10.1002/esp.1952

Zhang, Z., Walter, F., McArdell, B. W., Wenner, M., Chmiel, M., de Haas, T., & He, S. (2021). Insights from the particle impact model into the high-frequency seismic signature of debris flows. *Geophysical Research Letters*, *48*(1), e2020GL088994. https://doi.org/10.1029/2020gl088994

Zheng, H., Shi, Z., Yu, S., Fan, X., Hanley, K. J., & Feng, S. (2021). Erosion mechanisms of debris flow on the sediment bed. *Water Resources Research*, *57*(12), e2021WR030707. https://doi.org/10.1029/2021wr030707